NeuroImage 266 (2023) 119830

Contents lists available at ScienceDirect

NeuroImage

journal homepage: www.elsevier.com/locate/neuroimage

Organization of neurochemical interactions in young and older brains as revealed with a network approach: Evidence from proton magnetic resonance spectroscopy (^{1}H-MRS)

Geraldine Rodríguez-Nieto[a,1,*], Oron Levin[a,1], Lize Hermans[a], Akila Weerasekera[a,b,c], Anca Croitor Sava[b], Astrid Haghebaert[a], Astrid Huybrechts[a], Koen Cuypers[a,d,e], Dante Mantini[a,e], Uwe Himmelreich[b], Stephan P. Swinnen[a,e]

[a] Movement Control and Neuroplasticity Research Group, Biomedical Sciences, KU Leuven, Tervuurse Vest 101, Leuven 3001, Belgium
[b] Biomedical MRI Unit, Group Biomedical Sciences, KU Leuven, Belgium
[c] Department of Radiology, Harvard Medical School, Boston, MA, USA
[d] REVAL Research Institute, Hasselt University, Diepenbeek, Belgium
[e] Leuven Brain Institute, KU Leuven-LBI, Leuven, Belgium

ARTICLE INFO

Keywords:
Aging
Magnetic resonance spectroscopy
Graph theory
Metabolites
Networks
Choline

ABSTRACT

Aging is associated with alterations in the brain including structural and metabolic changes. Previous research has focused on neurometabolite level differences associated to age in a variety of brain regions, but the relationship among metabolites across the brain has been much less studied. Investigating these relationships can reveal underlying neurometabolic processes, their interdependency, and their progress throughout the lifespan. Using ^{1}H-MRS, we investigated the relationship among metabolite concentrations of N-acetylaspartate (NAA), creatine (Cr), choline (Cho), myo-Inositol (mIns) and glutamate-glutamine complex (Glx) in seven voxel locations, i.e., bilateral sensorimotor cortex, bilateral striatum, pre-supplementary motor area, right inferior frontal gyrus and occipital cortex. These measurements were performed on 59 human participants divided in two age groups: young adults (YA: 23.2 ± 4.3; 18–34 years) and older adults (OA: 67.5 ± 3.9; 61–74 years). Our results showed age-related differences in NAA, Cho, and mIns across brain regions, suggesting the presence of neurodegeneration and altered gliosis. Moreover, associative patterns among NAA, Cho and Cr were observed across the selected brain regions, which differed between young and older adults. Whereas most of metabolite concentrations were inhomogeneous across different brain regions, Cho levels were shown to be strongly related across brain regions in both age groups. Finally, we found metabolic associations between homologous brain regions (SM1 and striatum) in the OA group, with NAA showing a significant correlation between bilateral sensorimotor cortices (SM1) and mIns levels being correlated between the bilateral striata. We posit that a network perspective provides important insights regarding the potential interactions among neurochemicals underlying metabolic processes at a local and global level and their relationship with aging.

1. Introduction

Proton magnetic resonance spectroscopy (^{1}H-MRS) is a well-established neuroimaging technique that allows *in-vivo* quantification of neurometabolic differences in brain tissue as a function of age, disease or treatment (Cichocka and Bereś, 2018; Duarte et al., 2012; Gao et al., 2013; Grachev and Apkarian, 2001; Ion-Mărgineanu et al., 2017; Jones and Waldman, 2004; Lin and Rothman, 2014; Tumati et al., 2018; Waragai et al., 2017; Zhong et al., 2014). In healthy older adults, brain neurometabolites assessed with ^{1}H-MRS frequently show age-related declines in regional levels of N-acetylaspartate (NAA), gamma-aminobutyric acid (GABA), and glutamate-glutamine complex (Glx) and elevation in regional levels of choline (Cho) and myo-Inositol (mIns). However, null findings or the opposite pattern have also been reported which might be due to differences in the region and the tissue being measured (i.e., gray matter, white matter and/or cerebrospinal fluid; for a review see Cleeland et al. 2019). These neurometabolic alterations have been associated with declines in motor and cognitive functioning (Hermans et al., 2018; Levin et al., 2019; Marenco et al., 2018; Simmonite et al., 2019; Weerasekera et al., 2020;

* Corresponding author.
E-mail address: geraldine.rodrigueznieto@kuleuven.be (G. Rodríguez-Nieto).
[1] Shared first authorship.

https://doi.org/10.1016/j.neuroimage.2022.119830.
Received 28 July 2022; Received in revised form 19 October 2022; Accepted 21 December 2022
Available online 22 December 2022.

Zahr et al., 2013). Furthermore, age-dependent differences in brain neurochemical characteristics that are typically associated with aging, such as decreased levels of NAA and increased levels of Cho and mIns, can underlie important structural and physiological changes. These can refer to deterioration in axonal and myelin integrity (Ding et al., 2008; Grossman et al., 2015; Wijtenburg et al., 2013), gray matter loss (e.g., Ding et al. 2016), compromised neurotransmission (Cuypers and Marsman, 2021; Verstraelen et al., 2021) and/or systemic inflammation (Lind et al., 2021; Vints et al., 2022).

Age-related differences in neurometabolite concentrations can occur simultaneously or independently throughout different brain regions (Angelie et al., 2001; Cichocka and Bereś, 2018; Cleeland et al., 2019; Ding et al., 2016; Eylers et al., 2016; Haga et al., 2009; Levin et al., 2019; Pfefferbaum et al., 1999; Ross et al., 2006; Weerasekera et al., 2020). The synchronous changes among metabolites can signify particular alterations in general brain structural and/or functional properties. For instance, reduction of NAA levels and increase of mIns levels across multiple brain regions can generally be considered as biomarkers of demyelination and microstructural declines of WM tracts connecting these regions (e.g., Wijtenburg et al. 2013). The interplay between excitatory and inhibitory neurometabolites, along with different metabolite concentration levels, has also been tackled to disentangle the dynamics of physiological and behavioral processes (Cuypers and Marsman, 2021). Finally, the use of a ratio between two neurometabolites has often provided different insights in relation to the concentrations of a single metabolite absolute value (Cleeland et al., 2019; Weerasekera et al., 2020), showing again the importance of studying their association.

Noticeably, different brain regions may have particular metabolic signatures due to differences in the rate of neurodegeneration or functional characteristics. Previous studies showed that age-related differences in NAA, mIns, and Cho - which have been associated with neuronal loss and increased glial activity - were found to be prominent across different brain regions (e.g., Ding et al. 2016, Lind et al. 2020, Vints et al. 2022, Weerasekera et al., 2020), whereas age-related differences in Glx and GABA - that are functional biomarkers for motor and/or cognitive deficits - often exhibited region-specific trajectories (Hermans et al., 2018; Mase et al., 2021; Weerasekera et al., 2020).

Due to long MRS acquisition times, age-related alterations were typically reported from one or only a few brain regions in previous studies, hampering a network neurometabolic perspective. While the relationship among different metabolites has been investigated within constrained regions (typically through the ratio computations between two metabolites), little is known about the association among metabolites across more brain regions, and how consistent these patterns are throughout the lifespan. Studies aimed at addressing these questions may deepen our understanding of the metabolic properties and the changes underlying functional and structural brain architecture. Furthermore, a network perspective can reveal whether age-related metabolic alterations are region-specific or generic. The effect of aging on the organization of the brain's neurochemical networks was documented for the first time by Grachev and colleagues (Grachev et al., 2001; Grachev and Apkarian 2001) who examined age-related differences in the patterns of correlations between neurometabolic concentrations from multiple brain regions. Although this study yielded meaningful patterns regarding neurochemical organization, the authors did not correct for tissue volume, which compromises the interpretation of the results. Moreover, novel MR hardware (higher field strength, better shimming, water suppression, etc.) and MRS pulse sequences have substantially improved the data quality (better signal-to-noise ratio, spectral resolution and localization) over the past two decades.

Our study aimed to systematically examine age-related differences in the neurochemical organization of the brain by identifying specific correlation patterns among five neurometabolites (NAA, Cho, Cr, Glx and mIns; selected on the basis of aging literature) within and among seven brain regions that were considered to be involved in motor control processes pertaining to action execution and inhibition of action, more specifically: the left and right sensorimotor cortex (lSM1 and rSM1), the pre-supplementary motor area (preSMA; centered at the sagittal midline), the left and right striatum (lSTR and rSTR), the right inferior frontal gyrus (rIFG), and the occipital cortex (OCC; centered at the sagittal midline). Our main objective was to explore detailed features of neurometabolic organization within and across regions as well as age-related differences. First, we anticipated to replicate and extend previous studies regarding age-related neurometabolic concentrations showing lower NAA and Glx and higher mIns and Cho in older as compared to young adults (Angelie et al., 2001; Cichocka and Bereś, 2018; Cleeland et al., 2019; Ding et al., 2016; Eylers et al., 2016; Haga et al., 2009; Levin et al., 2019; Pfefferbaum et al., 1999; Ross et al., 2006; Weerasekera et al., 2020). Second, we investigated whether these differences are region specific. Third, as late adulthood has been characterized by a reduction of functional selectivity and decreased functional network segregation (Edde et al., 2021; King et al., 2018), and in concordance with previous neurochemical organization evidence (Grachev and Apkarian, 2001), we hypothesized that older adults would show stronger neurometabolic covariations across the brain than younger adults.

2. Methods

2.1. Participants

We included 30 young adults (age range: 18.3–33.8 years) and 29 older adults (age range, 60.2–73.8 years) that were from the same pool of participants as in Hermans et al. (2018) and Weerasekera et al. (2020). All participants were right-handed (Oldfield, 1971), had no past or present history of neurological or psychiatric disorders, no contraindications for magnetic resonance imaging (as indicated in the guidelines of the University Hospital Leuven), normal or corrected-to-normal vision, and reported no consumption of psychoactive medications at the time of the study. The experimental protocol was approved by the local Medical Ethics Committee for Biomedical Research (University Hospital Leuven; approval number S58333), and written informed consent was obtained from all participants prior to their inclusion in the study. Two older adults who scored less than 22 on the Montreal Cognitive Assessment (MoCA) test (Nasreddine et al., 2005) were excluded from the study and four participants were excluded for having incomplete datasets due to defective signal for particular metabolites. The final sample consisted of 53 participants: 29 young adults (mean age=23.15, sd=4.36, range=18–34) and 24 older adults (mean age=67.35, sd=3.76, range=61–74).

2.2. MRI and ^{1}H-MRS acquisitions

MRI and ^{1}H-MRS acquisitions were performed on a Philips 3T Achieva Dstream System (Philips Healthcare) equipped with a 32-channel receiver head coil. The imaging protocols used for acquisition were similar to those reported by Hermans et al. (2018) and Weerasekera et al. (2020). MR images were acquired using a high-resolution 3D T1-weighted structural image (3D turbo field echo (TFE); repetition time (TR) = 9.6 ms; echo time (TE) = 4.6 ms; resolution = 0.98 × 0.98 × 1.2 mm^3; 185 coronal slices) to obtain a 3D magnetization prepared gradient echo (MPRAGE). We used single-voxel MRS instead of MRSI (which has the advantage of measuring different regions simultaneously with a shorter scanning time), as this method has a higher signal to noise ratio and allows higher reliability in the spectra acquisition (Al-Iedani et al., 2017; Posse et al., 2013). The ^{1}H-MR spectra were acquired using the MEGA-PRESS spectral editing method (Mescher et al., 1998) with the following acquisition parameters: 14 ms editing pulses at 7.46 ppm (edit-OFF) and 1.9 ppm (edit-ON); TE = 68 ms; TR = 2 s; 320 averages; 2 kHz spectral width; MOIST (multiple optimizations insensitive suppression train) water suppression, re-

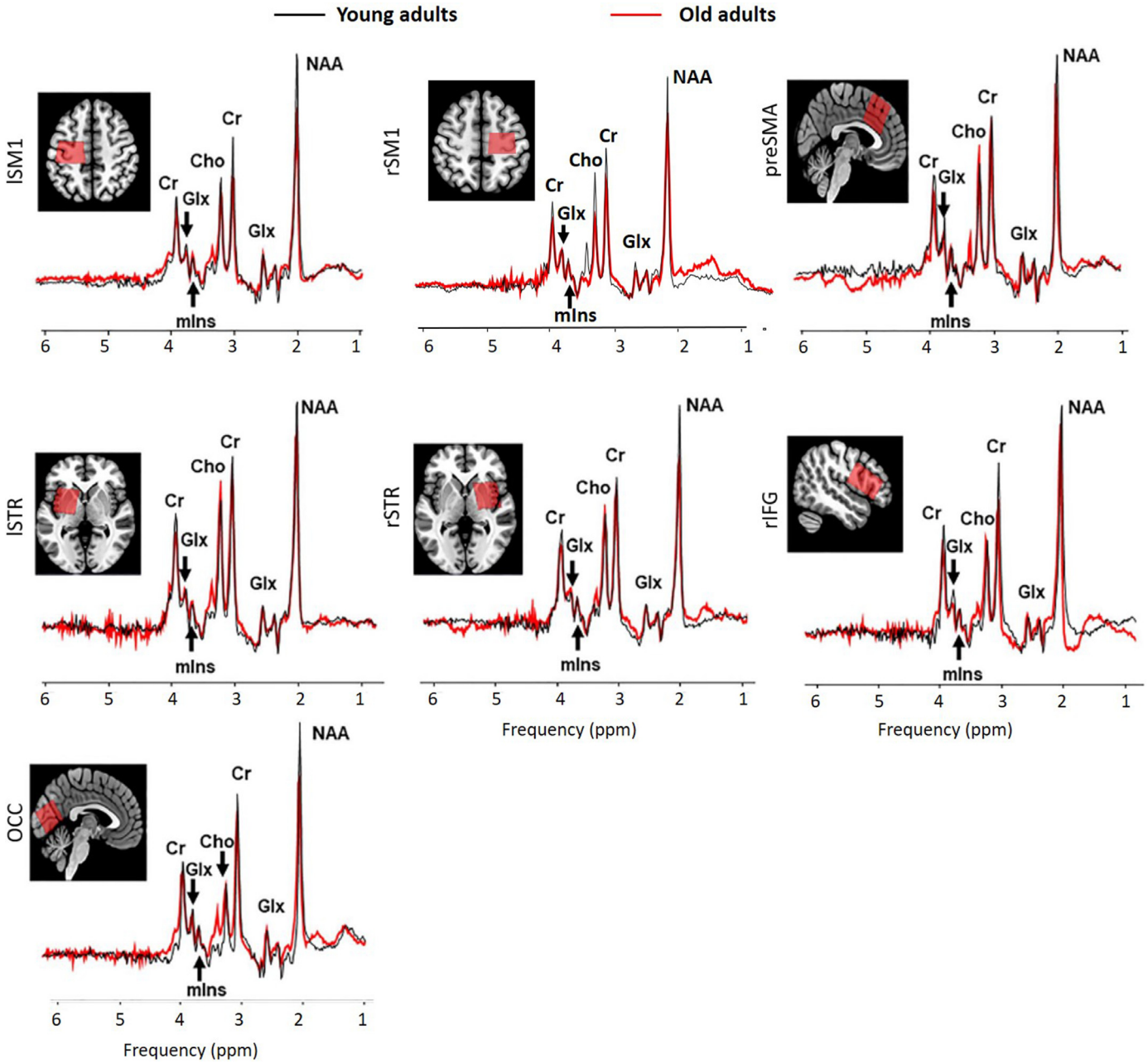

Fig. 1. Visual representation of voxel positions from: lSM1 and rSM1 (left and right sensorimotor cortex), preSMA (pre-supplementary motor area centered at the sagittal midline), lSTR and rSTR (left and right striatum), rIFG (right inferior frontal gyrus) and OCC (occipital cortex centered at the sagittal midline). Line graphs show the average spectra from young (black line) and older participants (red line). NAA – N-acetylaspartate; Cho – Choline, phosphocholine and glycerophosphocholine; Cr – Creatine and phosphocreatine; Glx – Glutamate and glutamine; and mIns – myo-Inositol.

sulting in an acquisition time of ~11 min per voxel. Unsuppressed water scans were acquired from all volumes of interest for absolute metabolite quantification in an interleaved manner, using the same acquisition parameters except for the number of averages of 16. Voxels were: (i) lSM1 and rSM1 (both voxel sizes: 3 × 3 × 3 cm), (ii) preSMA, obtained by a single voxel centered at the sagittal midline (size: 3 × 3 × 3 cm), (iii) lSTR and rSTR (both voxel sizes, 3 × 3 × 3 cm), (iv) rIFG (voxel size: 4 × 2.5 × 2.5 cm), and (v) OCC, obtained by a single voxel centered at the sagittal midline (size: 3 × 3 × 3 cm). Voxel positions are shown in Fig. 1 alongside the average spectra.

The acquisition of MR spectra started with a long high-resolution T1-weighted MRI scan (see above) followed by three ^{1}H-MRS scans and a short time break (10 min) outside the scanner. Next, a shorter low-resolution T1-weighted MRI scan (3D TFE; TR = 9.6 ms; TE = 4.6 ms; resolution = 1.2 × 1.2 × 2 mm^3; 111 coronal slices) and two ^{1}H-MRS scans were applied followed by a second 10 min break outside the scanner, a second short T1-weighted MRI scan, and two additional ^{1}H-MRS scans. The obtained T1-weighted MR anatomical images were used for the anatomical positioning of the voxels. The order of ^{1}H-MRS spectra acquisition from the different voxels were counterbalanced across participants, except for the lSTR that was followed by the rSTR or vice-versa. The voxels on the left and right SM1 were located centrally over the left and right-hand knob (Yousry et al., 1997), parallel to the anterior-posterior axis, with one surface parallel to the cortical surface in the coronal and axial views (Greenhouse et al., 2016). For the preSMA voxel, a horizontal line was drawn between the anterior commissure (AC) and

the posterior commissure (PC) in the sagittal plane, and a perpendicular line was drawn to this line through the AC. The preSMA voxel was centered over the median line with the posterior superior corner intersecting the perpendicular line (Kim et al., 2010). Subsequently, it was aligned with the cortical surface in the sagittal view. The rIFG voxel was placed centrally, on top of the right inferior frontal gyrus with the longitudinal axis placed in anteroposterior direction and parallel to the cortical surface. The striatal voxels (lSTR and rSTR) were positioned over the putamen and part of the caudate. The OCC voxel was positioned parallel with the cerebellar tentorium in the sagittal plane and placed as posterior and median as possible (Puts et al., 2011).

2.3. MRS quantification and image processing

Metabolites were quantified from the edit-OFF spectra (e.g., Maddock et al. 2018). Spectra from four of the 57 participants (one young adult and three older adults) were excluded from the final analyses due to poor quality of MRS acquisition. Therefore, data for quantification included 203 spectra (= 7 voxels × 29 participants) from young adults and 168 spectra (= 7 voxels × 24 participants) from older adults. For quality assessment, signal-to-noise ratios (SNR) were determined by jMRUI QUEST (v6.0) in the time-domain (maximum of FID/standard deviation of FID tail) (Stephan et al., 2009). Only spectra with linewidths less than 10 Hz and SNR greater than 5 were included for quantification. All spectra were visually inspected to ensure the absence of artifacts. Following this screening procedure, 16 spectra were excluded and were eliminated from further analyses, consisting of two spectra from one younger adult and 14 spectra from three older adults. Water-referenced concentrations of NAA (N-acetylaspartate), Glx (glutamate and glutamine), Cr (creatine and phosphocreatine), Cho (choline, phosphocholine and glycerophosphocholine), and mIns (myo-Inositol) were then quantified for each of the seven voxel locations and were included in further processing. Next, SPM8 (http://www.fil.ion.ucl.ac.uk/spm/) was utilized to create segmentations from the MPRAGE T1-weighted MR images, acquired for the localization and placement of the MRS voxel. Voxel registration was executed using MATLAB (The MathWorks, Natick, Massachusetts, USA) custom-made scripts (Sanaei Nezhad et al., 2017). The scripts created a binary mask of the voxel location using the T1-weighted MR image and the orientation and location information from the Philips SPAR files. Subsequently SPM8 was used to segment the T1-weighted MR image into gray matter (GM), white matter (WM) and cerebrospinal fluid (CSF) and calculate the respective partial volume fractions within the binary mask. SPM uses a diffeomorphic algorithm to warp individual subject images into MNI space and generate spatially normalized and smoothed Jacobian scaled images, thereby normalizing the WM and GM sensitivities in the T1-weighted MR images. By using this technical procedure, the percentages of each tissue type within the seven voxels could be calculated and percentages of GM, WM and CSF were obtained. These tissue fractions were then used to correct for metabolite concentrations and, with the use of QUEST, for differences in CSF content (Gasparovic et al., 2006). We used T1 values of 1331 ms for GM, 832 ms for WM, and 3817 ms for CSF to calculate the final corrected metabolite concentrations. The used T2 values were 110 ms (GM), 79 ms (WM), and 503 ms (CSF). Relaxation times were taken from Wansapura et al. (1999) and Träber et al. (2004). From this dataset, GABA concentrations were also extracted, processed and analyzed; the results related to this metabolite can be found in Hermans et al. (2018).

2.4. Statistical analysis

Variables of interest were the water-referenced tissue-corrected metabolite concentration measures of the five neurometabolites (NAA, Cho, Cr, Glx and mIns) from the seven voxel locations (lSM1, rSM1, preSMA, lSTR, rSTR, rIFG and OCC). Group differences in neurometabolite concentrations between young and older adults were evaluated with a series of Student's t-tests and p-values were corrected for multiple testing using the Benjamini–Hochberg false discovery rate (FDR) method (Benjamini and Hochberg, 1995); see supplemental Table S1.

Thereafter, we conducted Pearson correlation analyses among the five metabolites from the seven regions and corrected them for multiple comparisons (uncorrected correlations can be consulted in the supplementary material). Cook's Distance (CD) analysis was used to control

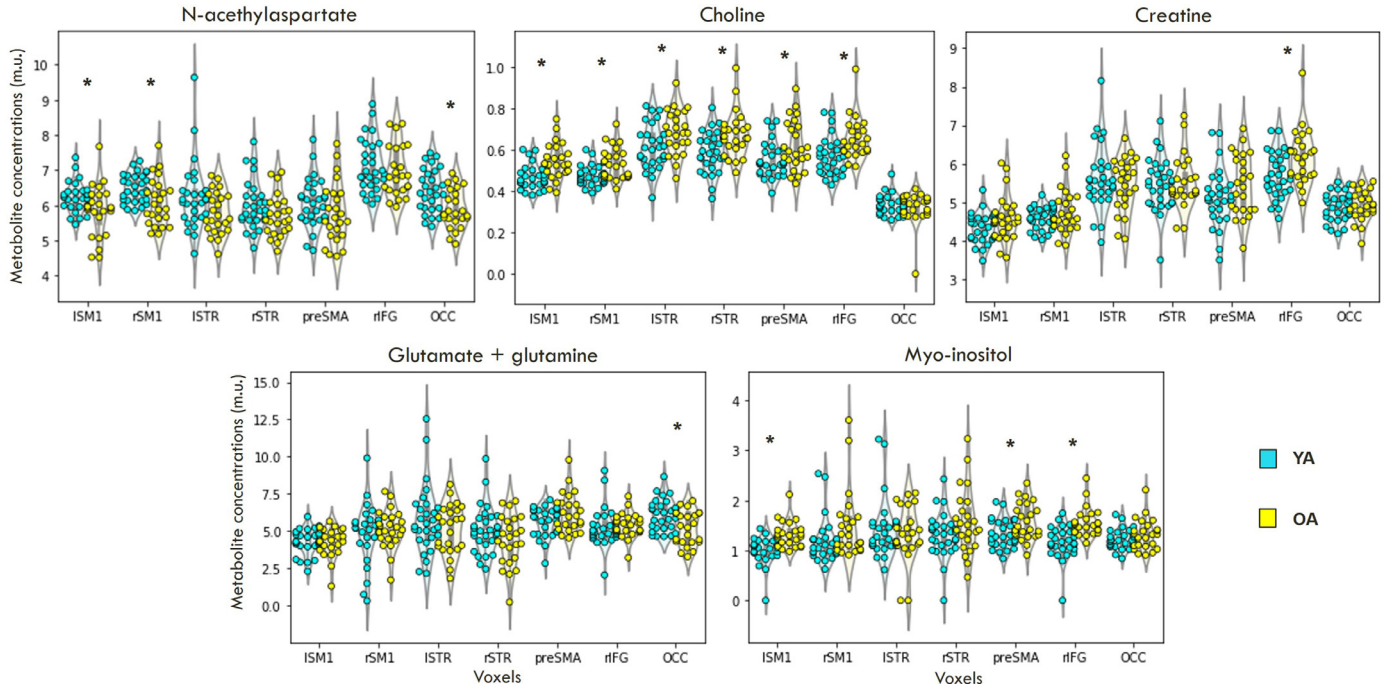

Fig. 2. Metabolite concentrations for young (blue) and older (yellow) adults in the seven voxels of interest: lSM1 and rSM1 (left and right sensorimotor cortex), preSMA (pre-supplementary motor area centered at the sagittal midline), lSTR and rSTR (left and right striatum), rIFG (right inferior frontal gyrus) and OCC (occipital cortex centered at the sagittal midline). Asterisks point to significant differences between age groups (after FDR correction). m.u. – molar units.

for outliers that have a great influence on the correlations, with a cut-off value of CD > 1 (Stevens, 1984). We obtained one correlation matrix per voxel (correlations of different metabolites within each voxel – intraregional cross-metabolites network) and one correlation matrix per metabolite (correlations of the same metabolite across the seven voxels – interregional within-metabolite network), for the total sample and for each age group. The correlations from the intraregional cross-metabolites matrices were controlled for gray matter, white matter and cerebrospinal fluid volumes. For interregional within-metabolite matrices, the correlations were only controlled for the gray matter volume from the two regions pertinent to each correlation. We did not control for white matter or CSF as doing so would have amounted to six control variables (three volume values per region) which was undesired with our sample size (Field, 2013). The correlations within each matrix were corrected for multiple comparisons through FDR.

From the interregional within-metabolites and intraregional cross-metabolites networks a connectivity degree index was extracted. Within the framework of Graph Theory, the connectivity degree is defined as the number of edges (in this case significant correlations after FDR correction) within a particular network and is indicative of the *richness of interactions or relation among the nodes (metabolites) of a network*. The connectivity degree of a particular network is the average of the connectivity degree from all the nodes in that network. From here on, we will use the term *network connectivity or connectivity degree* to refer to this index (or connections to refer to the presence of edges), which indicates the presence of statistically significant correlations. Such correlations suggest common properties of the system, which may represent common physiological or structural phenomena in intraregional cross-metabolic connectivity and potentially relate to brain structural or functional connectivity in the case of interregional within-metabolite connectivity.

In order to compare whether the correlations from young and older participants were significantly different, the correlation coefficients were converted to z scores through the Fisher transformation method, compared through t-tests and corrected for multiple comparisons using FDR. The threshold significance level was set at 0.05 for all analyses unless otherwise specified.

All independent sample t-tests and partial correlations were conducted with the software SPSS (v.28.0.1.0; IBM Corp. 2021); multiple comparisons corrections (FDR) were calculated within Excel, and Pearson to Fisher coefficients transformations were calculated with a Python 3.7 script using the Numpy and Pandas libraries (Harris et al., 2020; McKinney et al., 2010). The connectivity degree analyses, network figures and heatmaps were generated with the NetworkX and Matplotlib Python libraries (Hagberg et al., 2008; Hunter, 2007).

3. Results

3.1. Age–related differences in neurometabolite concentrations across regions

As compared to young adults, older adults showed significantly higher levels of Cho (bilateral SM1, bilateral striatal areas, preSMA and rIFG; FDR-corrected ps < 0.05) and mIns (lSM1, preSMA, and rIFG; FDR-corrected ps < 0.05) and significant reductions of NAA (bilateral SM1 and OCC; FDR-corrected ps < 0.05); for group means and p-values see Supplemental Table S1. In addition, we observed a significantly lower levels of Glx in the OCC area (FDR-corrected $p = 0.02$) and significantly higher levels of Cr in the rIFG (FDR-corrected $p < 0.01$) in older as compared to young adults (Fig. 2). Taken together, our findings indicate that age-related neurometabolic alterations were characterized primarily by a general increase in levels of Cho. The remaining group differences (i.e., higher levels of mIns and Cr and lower levels of NAA with age) were inconsistent across the seven voxels, indicating that age-related differences in levels of NAA, mIns, Glx and Cr appear to be more regional specific.

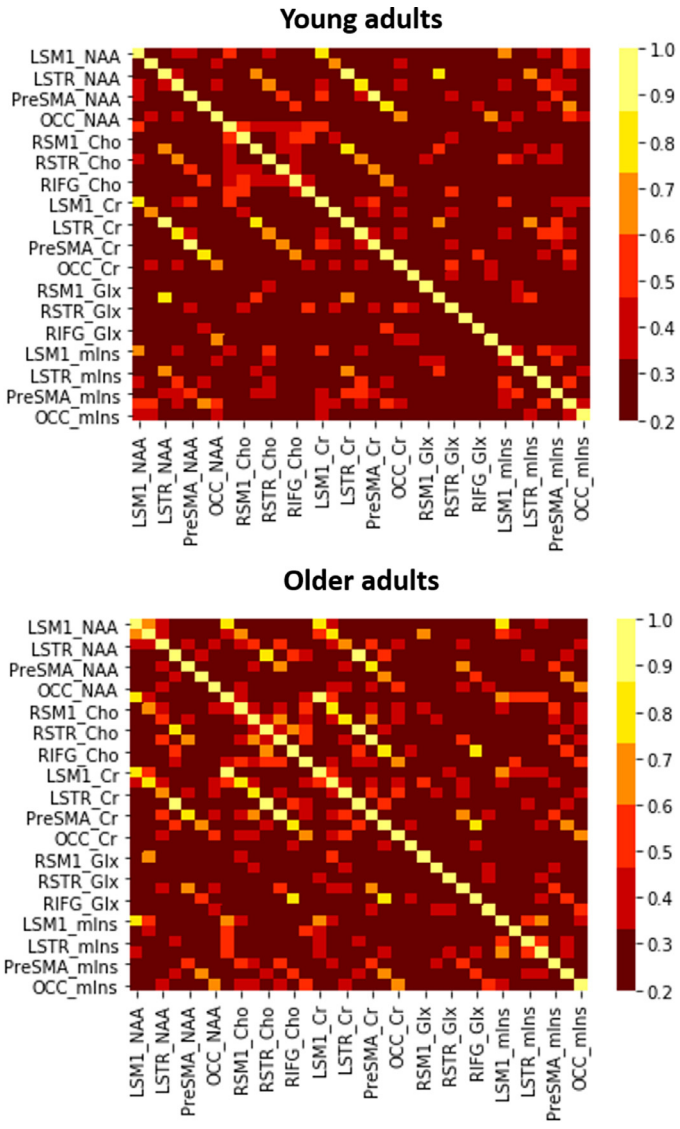

Fig. 3. Heatmaps representing correlations among the five metabolites from the seven voxels (before controlling for GM, WM and CSF volumes and before multiple comparisons correction) in young (top) and older (bottom) participants. The order of voxels is: lSM1, rSM1, lSTR, rSTR, preSMA, rIFG and OCC. For visualization purposes the labels are only shown for half of the nodes in an intercalated manner.

3.2. The neurochemical network

The heatmaps representing correlations among the five metabolites from the seven voxels before controlling for tissue volume (GM, WM and CSF) and before correcting for multiple comparisons are depicted for young (Fig. 3A) and older (Fig. 3B) participants. Graphical representations showing the associations among the five neurometabolites within and across the seven voxels (inter- and intraregional networks together; after controlling for tissue volume and after multiple comparisons correction) are depicted for the full sample and for the young and older adult groups separately (Fig. S1).

3.2.1. Neurometabolic associations across regions

Fig. 4 depicts the interregional within-metabolite networks for the full sample. The correlation matrices from these networks (for each sample) and network figures for young and older adults can be consulted in the Supplementary Materials (Tables S3, S5 and S7; Fig. S2). Overall, it can be seen that Cho exhibited the most spread interregional network

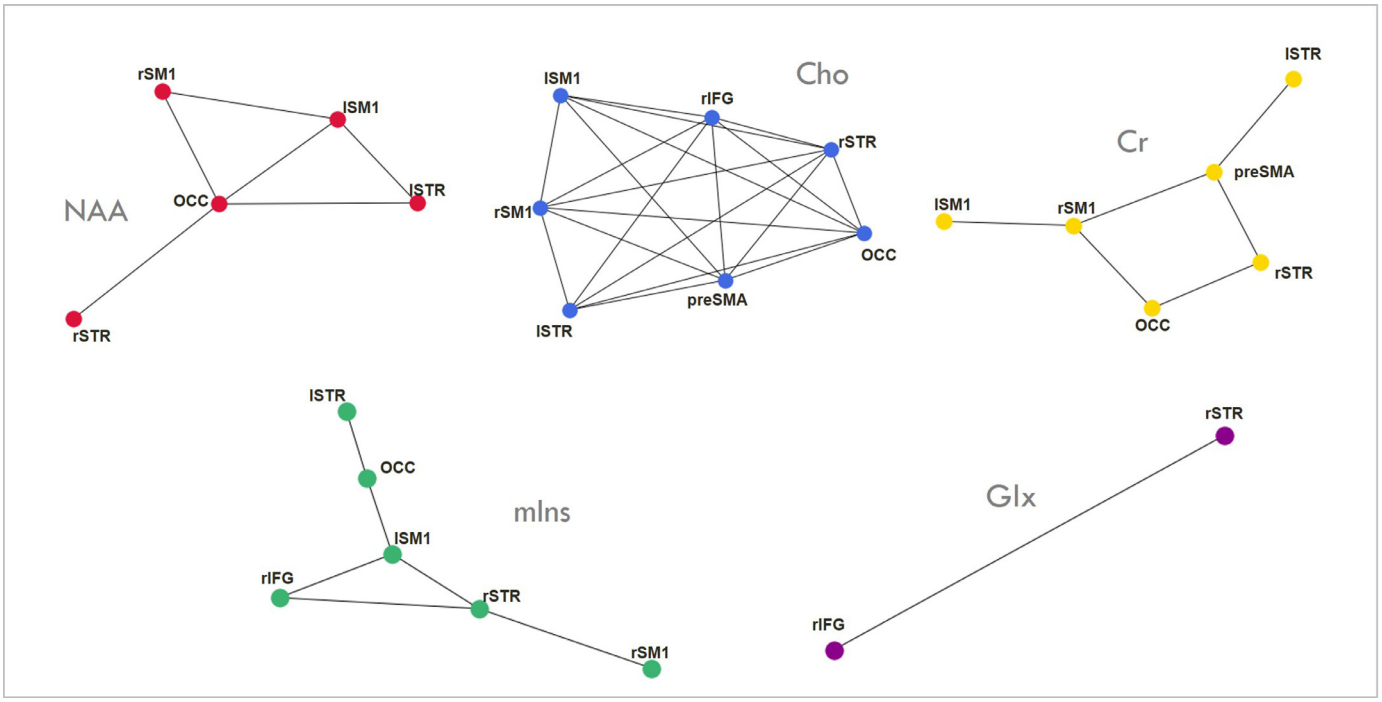

Fig. 4. Interregional networks for each metabolite. Metabolites: NAA – N-acetylaspartate; Cho – choline; Cr – creatine; mIns – myo-Inositol and Glx – glutamate. Voxels of interest: lSM1 and rSM1– left and right sensorimotor cortex; preSMA –pre-supplementary motor area centered at the sagittal midline; lSTR and rSTR – left and right striatum; rIFG – right inferior frontal gyrus; and OCC – occipital cortex centered at the sagittal midline.

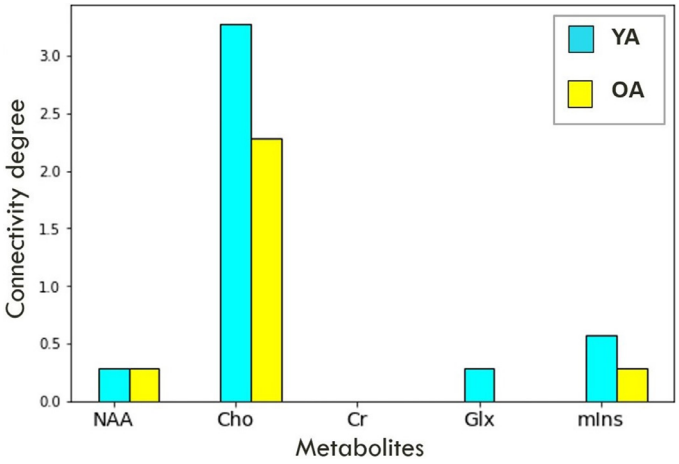

Fig. 5. Connectivity degree from interregional networks is shown for young and older adults. No correlations survived multiple comparisons correction for the Cr networks in both samples, nor for the Glx network in the older adult sample.

connectivity with a higher number of connections (20 of 21 interactions; $p \leq 0.006$; connectivity degree = 5.71, Fig. 4) and Glx the least (1 of 21 interactions; $p \leq 0.007$; connectivity degree = 0.28, Fig. 4). NAA (6 of 21, $p \leq 0.01$; connectivity degree = 1.71, Fig. 4), Cr (6 of 21, $p \leq 0.01$; connectivity degree = 1.71, Fig. 4), and mIns (6 of 21, $p \leq 0.007$; connectivity degree = 1.71, Fig. 4) were positioned in between. The most frequent associations were observed between the bilateral SM1 regions (for NAA, Cho, and Cr; all $p \leq 0.001$), between OCC and lSM1, rSM1 and rSTR (for NAA and Cho; all $p \leq 0.01$) and between preSMA and rSM1, rSTR and lSTR (for Cho and Cr; all $p \leq 0.006$).

When subdivided by age group, the main difference was observed for Cho, showing a lower connectivity degree in older individuals (young = 3.28, older = 2.28) (Fig. 5). The connectivity degree was slightly lower for the Glx and mIns in older participants (Glx: young = 0.28, older = 0; mIns: young = 0.57, older = 0.28; Fig. 5).

Among the statistical differences that survived FDR in interregional within-metabolites correlations, older adults showed a stronger correlation between the NAA concentrations of the bilateral SM1, and also between the mIns concentrations of the bilateral striatum and between lSM1 and lSTR (Table S2).

3.2.2. *Neurometabolic associations within regions*

Fig. 6 depicts the intraregional cross-metabolites networks for the full sample. The correlation matrices from these networks and the network maps for young and older adults can be consulted in the Supplementary Materials (Tables S4, S6 and S8; Fig. S3). The connectivity degree for each of the intraregional cross-metabolites networks is displayed in Fig. 7 for the two age groups. Older adults showed a higher intraregional metabolic connectivity in the preSMA. Although this pattern was also observed in the bilateral SM1 and rIFG, significant correlation differences among young and older adults were mostly observed in the preSMA (after FDR; Table S2). As can be seen from Fig. 6, intraregional neurometabolic interactions for the whole sample were characterized primarily by significant correlations among Cho, NAA, and Cr in all voxels except for OCC. These interactions followed a triangle graph fashion, i.e., each of the three neurometabolites was significantly correlated with the other two neurometabolites (except in RIFG where NAA and Cho levels were not correlated). Other connections were observed for NAA-mIns-Cr (lSM1, lSTR, preSMA, and rIFG) and NAA-Glx-Cr (lSTR, preSMA, rIFG). To determine whether pairwise correlations within the Cho-NAA-Cr intraregional associations were masked by common correlations with the third metabolite we calculated the partial correlations for NAA-Cho, Cho-Cr, and NAA-Cr while controlling for Cr, NAA, and Cho, respectively (Table S9). In all seven voxels, we observed significant positive correlations for Cho-Cr when controlling for NAA (all Rs > 0.58) and NAA-Cr when controlling for Cho (all Rs > 0.61); all uncorrected ps < 0.001. However, when controlling for Cr, the correlations between NAA and Cho turned from significantly positive ($R = 0.52$, $p < 0.001$) to non-significant ($R = -0.18$, $p = 0.21$) in the lSM1 and

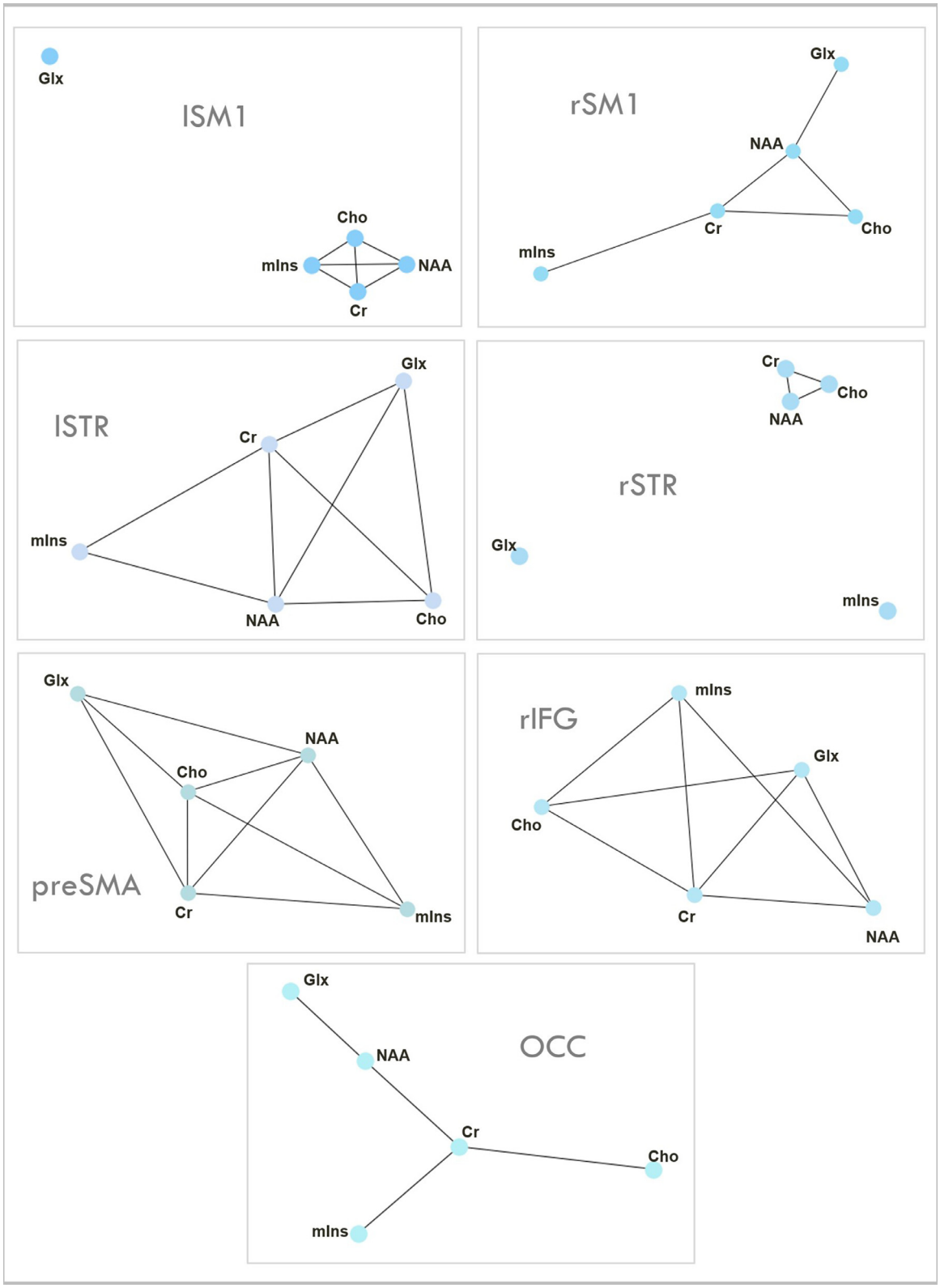

Fig. 6. Intraregional cross-metabolite networks for the full sample. Voxels of interest: lSM1 and rSM1– left and right sensorimotor cortex; preSMA – pre-supplementary motor area centered at the sagittal midline; lSTR and rSTR – left and right striatum; rIFG – right inferior frontal gyrus; and OCC – occipital cortex centered at the sagittal midline. Metabolites: NAA – N-acetylaspartate; Cho – choline; Cr – creatine; mIns – myo-Inositol and Glx – glutamate.

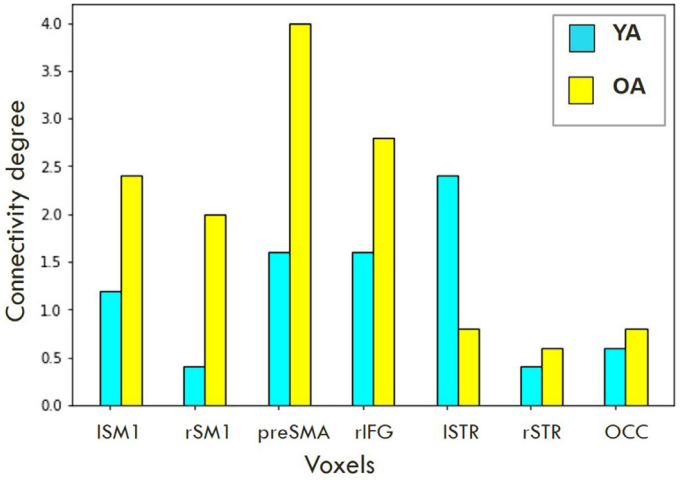

Fig. 7. Connectivity degree from intraregional cross-metabolite networks for young and older adults.

turned from positive (all Rs > 0.33 in rSM1 and rSTR) or non-significant (in rIFG and OCC) to significantly negative (all Rs < −0.27) (all uncorrected ps < 0.05). Only the NAA-Cho correlations remained significant in the preSMA and lSTR regions after controling for Cr (both Rs > 0.34, $p<0.015$). Our tentative conclusion is that interactions among Cho, NAA, and Cr may be driven primarily by levels of Cr.

4. Discussion

We examined the effect of typical aging on the neurochemical organization of the brain by exploring the associations among neurometabolites (NAA, Cho, Cr, Glx, and mIns) within and across a set of brain regions including the bilateral sensorimotor cortices (lSM1 and rSM1), the bilateral striatal areas (lSTR and rSTR), the preSMA, the rIFG, and the OCC. In line with previous studies, we found lower levels of NAA and higher levels of Cho and mIns across different regions in older participants (for a review see Cleeland et al. 2019). Our network analysis uniquely revealed that older adults had a stronger intraregional neurometabolic connectivity, suggesting the co-participation of these metabolites in neurodegenerative and possibly de-segregation processes. Choline showed to be strongly correlated across different brain regions in young and older participants while NAA, Cho and Cr were commonly interrelated within different brain regions. Taken together, these findings suggest a moderate age-related difference in the neurochemical organization of the brain.

4.1. Effects of aging on neurometabolic concentrations

In line with previous findings our observations showed lower levels of NAA and higher levels of Cho and mIns in older participants across different brain regions (Cichocka and Bereś, 2018; Cleeland et al., 2019; Marjanska et al., 2017; Sailasuta et al., 2008; Suri et al., 2017; Yang et al., 2014). These neurometabolic differences are thought to reflect age-related neuronal density decrease and demyelination (NAA), increased glial cell activity (mIns), and membrane alterations (Cho), among others (e.g., Chiu et al. 2014, Ding et al. 2016, Eylers et al. 2016, García Santos et al. 2010, Lind et al. 2021, Moffett et al. 2007, Vints et al. 2022, Weerasekera et al. 2020, for a review see Cleeland et al. 2019).

In our study, the age-related differences of NAA were more prominent in the bilateral SM1 and OCC cortices. NAA has been related to neuronal mitochondrial function, myelin turnover and neuronal density (Moffett et al., 2007; Paslakis et al., 2014). Consequently, the observed differences in NAA may be related to functional changes in neural bioenergetic demands and/or decreased neuronal density. Choline was consistently higher across regions in the older as compared to the young adults, with the exception of OCC where both groups did not differ. The Cho concentrations observed from MRS have been partially attributed to cell membrane breakdown (Katz-Brull et al., 2002) and elevated Cho in the aging brain appears to be a marker of brain inflammation, demyelination, gliosis and cognitive decline (Harris et al., 2014; Lind et al., 2020; Vints et al., 2022). Finally, mIns was consistently higher in the older adults across all regions, although the difference was only significant in lSM1, preSMA and rIFG. This regional specificity may indicate that the increase in mIns is related to differences in local functional properties. mIns is a growth promoting factor and osmoregulator, used as a therapeutic agent in a wide range of diseases (Chhetri, 2019). Its increased presence in the aging brain might possibly be reflective of a compensatory mechanism to counterbalance neurodegenerative processes, which might be more accentuated in regions that are engaged in daily crucial activities (e.g., movement and cognitive control). More research is needed to confirm this tentative interpretation.

4.2. Effects of aging on neurometabolic interregional networks

Our working hypotheses assumed that older adults are prone to evolving into a more interconnected network which could be the outcome of general processes of brain dedifferentiation or common neurodegenerative or metabolic changes across multiple regions of the brain. However, the data revealed that NAA, Cr, Glx and mIns levels were poorly related across different regions in both age groups. Moreover, the few correlations found from these metabolites (between different brain regions) were inconsistent between the two age groups. The correlations among these metabolite concentrations across regions shows a distinct dispersion across the brain rather than a uniform distribution, thereby highlighting the importance of voxel selection in MRS studies and its consideration when comparing different studies for investigating its relationship with behavioral functions.

In contrast to these findings, Cho levels were highly correlated across the different regions and in both age groups. As mentioned earlier, Cho concentrations were higher in older adults in most of the studied regions and the correlations of Cho levels across the brain were comparable in both age groups. This homogeneity appears to suggest that Cho concentrations are mainly related to global mechanisms in both age groups. This global effect may be due to the fact that Cho is an essential component of all cell membranes (Tayebati et al., 2015). Therefore, the fact that the Cho levels were significantly higher in older adults in almost all regions (except in OCC) may suggest an association with structural age-related differences rather than with functional ones, as the effect of the latter (e.g., of choline as precursor of cholinergic neurotransmission) would be expected to be local (Schliebs and Arendt, 2011). In concordance with this, higher levels of Cho are generally considered to be the result of membrane breakdown (Klein, 2000).

We found that the older adults showed a significantly stronger correlation of NAA concentrations between the bilateral SM1. As previously mentioned, NAA concentrations were significantly lower in older adults in the bilateral sensorimotor cortex. NAA is related to bioenergetic metabolism in neurons and N-acetyl-aspartyl-glutamate (NAAG) –also measured under the NAA spectrum- is a neuromodulator and precursor of glutamate and NAA (Moffett et al., 2007; Castellano et al., 2012). Remarkably, the hemispheric lateralization of movement control observed in young individuals diminishes with age (Hutchinson et al., 2002; Inuggi et al., 2011) and a reduction in interhemispheric interactions has been suggested (Coppi et al., 2014; Mayhew et al., 2022). Thus, the decrease of NAA in the bilateral SM1 may be associated with these differences and the observed correlation between both areas in older adults but not young adults may be related to the bi-lateralization of movement control, possibly reflecting dedifferentiation processes. Alternatively, the synchronous NAA decrease in bilateral SM1, could be also reflective of demyelination or changes in osmoregulatory processes

(Moffet et al., 2007). These explanations are not mutually exclusive; however, we cannot infer causal or directional links nor exclude other possible mechanisms.

We also observed that older adults showed a significant and positive correlation of mIns concentrations between the bilateral striata, which was absent in young adults. Interestingly, the mIns absolute concentrations were not significantly different among young and older adults in the striata. Thus, although the mIns levels are not different among the two age groups, the correlation in the bilateral striatum in older adults could be indicative of a change in the mIns dynamics distinctive for late adulthood. As mentioned earlier, mIns could possibly be reflective of compensatory mechanisms during neurodegeneration.

4.3. Effects of aging on neurometabolic associations within regions

Although we did not detect major age-related differences in interregional connectivity, we observed differences in intraregional connectivity. In older adults, the different metabolites showed a higher interrelation among each other within the bilateral SM1, the rIFG and the preSMA. Nonetheless, the most prominent differences were found in the preSMA. Here, the Glx levels from the older sample showed a higher relation with Cr, mIns and NAA. This observation may suggest an increased involvement of Glx in metabolic pathways, such as those referring to NAA synthesis (Moffett et al., 2007), which could be triggered as a compensatory reaction to decreased expressions of NAA, NAAG and glutamate in the aging brain (Chiu et al., 2014). Another explanation is that age-related changes in the preSMA function (e.g., Coxon et al. 2016, Weerasekera et al. 2020) are associated to glutamatergic metabolic processes, either as a compensatory mechanism to preserve functionality or as a consequence of functional alterations. These tentative perspectives require further experimental verification.

We also observed an association between NAA and Cr across regions, which suggests their participation in common metabolic processes. We did not observe differences in the NAA-Cr associations between young and older, suggesting that this association is rather stable across adulthood and across regions. The NAA-Cr ratio has shown to be a diagnostic marker of long-term outcome in patients with stroke and hypoxia (Ross et al., 1998; Parsons et al., 2000). It is possible that the NAA-Cr relationship underlies the basal energetic demands of neurons and glia, as both metabolites are present in both types of cells (Urenjak et al., 1993).

In the full sample and in the older adults only, NAA and Cr concentrations were commonly associated with Cho as well. In the full sample, the Cho-Cr relationship was observed in all areas, and remained stable after controlling for NAA. In both age samples, the Cho-Cr relationship was present in the lSTR and in the preSMA. However, whereas the Cho-Cr correlation was strong in the bilateral sensorimotor cortices and rIFG in older participants, this relationship was absent in the younger adults (although this difference only remained significant in lSM1 after multiple comparisons correction). As Cr is involved in the generation of ATP, it is possible that the metabolic process underlying the Cho-Cr relationship relates to cholinergic communication (in contrast to structural differences which presumably relate mostly to Cho alone) either through acetylcholine transmission or neuromodulation. Therefore, age-related differences in the Cho-Cr relationship may reveal compensatory and/or adaptive mechanisms related to overcoming declines in movement control. For example, a previous study has shown that cholinergic deficits in sensorimotor areas are related to gait disturbances and an increased risk of falling in older adults (Pelosin et al., 2016).

The association between NAA and Cho was not stable across regions. When controlling for Cr levels, the NAA-Cho relation was no longer significant in the left SM1 and became a negative association in right SM1, right STR, rIFG and OCC in the full sample. In addition, the NAA-Cho association was more frequently observed in the older group, although the correlation difference between young and older individuals was only significant in the rSM1. It is possible that NAA and Cho commonly relate to Cr due to their co-participation in bioenergetic mechanisms. But when this common association with Cr is controlled for, the higher levels of NAA -an indicator of neuronal integrity- and low levels of Cho -an indicator of membrane breakdown- may indicate structural changes specific to the regions with negative correlations (right SM1, right STR, rIFG and OCC). Importantly, our findings are based on correlations accounting for GM, WM and CSF volumes. Thus, it is expected that age-related differences in these tissue volumes may not be the main contributing factors underlying the neurometabolic differences reported here.

4.4. General considerations and imitations

The present study is considered to be explorative and -to our best knowledge- involves an approach not used before, i.e., the implementation of network analyses to examine relationships among metabolites across different brain regions. Therefore, the interpretations of some of our results are tentative and should be considered with caution, given the limited literature that is currently available on this topic. Future multimodal and longitudinal studies and further technological advances in MRS are required to test the preliminary interpretations proposed here.

Furthermore, we emphasize that the correlations among metabolites concentrations strongly suggest common underlying properties, either physiological or structural. We have suggested one or the other according to the current knowledge in the field. As it currently stands, it is not possible to know with certainty which sort of mechanisms those metabolites are predominantly involved in when measured by MRS. However, the present approach may constitute and advance in our understanding of the properties and role of particular metabolites (e.g., involvement in local/global mechanisms, metabolites interactions, etc.). The introduced metabolic network approach may help elucidate physiological properties across development and pathologies that are not reachable through the use of other neuroscientific methods to study the human brain *in vivo*.

So far, it is not possible to acquire MRS measurements from remote brain regions simultaneously. The acquisition of the MRS at different time points for each of our voxels of interest and the strength of the observed correlations (revealing consistent co-variation across individuals) suggest that the relationships portrayed within the network analyses underlie commonalities in stable properties (either physiological or structural) and are not expected to be state-dependent. Other approaches, such as MRSI may be more suitable to test state-dependent metabolic networks. In addition, although MRSI has the limitation of not being able to measure remote brain areas, one advantage is a reduced voxel size limiting the diversity of structures and tissues (as compared to single voxel MRS), which may also be considered in future studies.

This study found a poor metabolic connectivity of Glx which may be due to a modest signal obtained from the present MRS sequence (MEGAPRESS, TE=68). In addition, given the excitatory function of this metabolite, it is expected that its concentrations adapt according to temporary states, therefore, future protocols may address the state-dependent connectivity of this metabolite.

Although our sample size is limited, the age-related differences in metabolites concentrations replicated previous findings (Section 4.1). Moreover, the network analyses only comprised strong correlations, which survived multiple comparisons correction and that were controlled for outliers. Similarly, when comparing the correlation coefficients between age groups, we also applied multiple comparisons correction. Although our conclusions were drawn from robust findings, a limited sample size also leads to an increased risk of Type II errors and our study may have been limited in detecting further age-related differences.

5. Conclusion

We investigated age-related differences in metabolite concentrations within and across distinct regions of the brain through a network ap-

proach. Besides neurochemical differences, the comparison between the young and older groups revealed a higher intraregional neurometabolic connectivity in older adults (local effect) but minor changes in interregional neurometabolic connectivity (global effect). From a local perspective, the correlation among different metabolites within a particular region or node suggests the common involvement of those neurochemicals in a particular biochemical process. In this respect, we suggest that some of the differences between the network metrics of young and older adults in focal brain regions may be indicative of, or attributed to neurodegenerative or compensatory mechanisms in the aging brain.

Funding

Funding was provided by: KU Leuven Research Fund (C16/15/070) to SS, DM and OL; the Fonds Wetenschappelijk Onderzoek – Vlaanderen (FWO) (G089818N) to SS and the FWO infrastructure grant to DM and SS; the Excellence of Science (EOS) grant from FWO and the Fonds de la Recherche Scientifique (FNRS) (EOS 30,446,199, MEMODYN) to SS and DM; and EC H2020-MSCA-ITN 2018 INSPiRE-Med (813,120) to UH.

Data and code availability statement

The database and the scripts used for this study can be consulted at: https://osf.io/c9p6q/?view_only=520ec7ba7b9e48a6b4be4318e34bbf3c.

Ethics statement

The experimental protocol was approved by the local Medical Ethics Committee for Biomedical Research (University Hospital Leuven; approval number S58333), and written informed consent was obtained from all participants prior to their inclusion in the study.

Declaration of Competing Interest

The authors declare no conflicts of interest.

Credit authorship contribution statement

Geraldine Rodríguez-Nieto: Conceptualization, Formal analysis, Writing – original draft, Writing – review & editing. **Oron Levin:** Conceptualization, Data curation, Funding acquisition, Supervision, Writing – original draft, Writing – review & editing. **Lize Hermans:** Data curation, Funding acquisition. **Akila Weerasekera:** Data curation. **Anca Croitor Sava:** Data curation. **Astrid Haghebaert:** Data curation. **Astrid Huybrechts:** Data curation. **Koen Cuypers:** Writing – review & editing. **Dante Mantini:** Funding acquisition, Writing – review & editing. **Uwe Himmelreich:** Funding acquisition, Writing – review & editing. **Stephan P. Swinnen:** Conceptualization, Funding acquisition, Supervision, Writing – review & editing.

Data availability

We have shared our resources through the OSF repository.

Supplementary materials

Supplementary material associated with this article can be found, in the online version, at doi:10.1016/j.neuroimage.2022.119830.

References

Al-Iedani, O., Lechner-Scott, J., Ribbons, K., Ramadan, S., 2017. Fast magnetic resonance spectroscopic imaging techniques in human brain-applications in multiple sclerosis. J. Biomed. Sci. 24 (1), 1–19.

Angelie, E., Bonmartin, A., Boudraa, A., Gonnaud, P., Mallet, J., Sappey-Marinier, D., 2001. Regional differences and metabolic changes in normal aging of the human brain: proton MR spectroscopic imaging study. Ann. J. Neuroradiol. 22, 119–127.

Castellano, G., Dias, C.S.B., Foerster, B., Li, L.M., Covolan, R.J.M., 2012. NAA and NAAG variation in neuronal activation during visual stimulation. Braz. J. Med. Biol. Res. 45, 1031–1036.

Chhetri, D.R., 2019. Myo-inositol and its derivatives: their emerging role in the treatment of human diseases. Front. Pharmacol. 10, 1172.

Chiu, P.W., Mak, H.K., Yau, K.K., Chan, Q., Chang, R.C., Chu, L.W., 2014. Metabolic changes in the anterior and posterior cingulate cortices of the normal aging brain: proton magnetic resonance spectroscopy study at 3 T. Age 36 (1), 251–264 (Omaha).

Cichocka, M., Bereś, A., 2018. From fetus to older age: a review of brain metabolic changes across the lifespan. Ageing Res. Rev. 46, 60–73.

Cleeland, C., Pipingas, A., Scholey, A., White, D., 2019. Neurochemical changes in the aging brain: a systematic review. Neurosci. Biobehav. Rev. 98, 306–319.

Coppi, E., Houdayer, E., Chieffo, R., Spagnolo, F., Inuggi, A., Straffi, L., et al., 2014. Age-related changes in motor cortical representation and interhemispheric interactions: a transcranial magnetic stimulation study. Front. Aging Neurosci. 6, 209.

Coxon, J.P., Goble, D.J., Leunissen, I., Van Impe, A., Wenderoth, N., Swinnen, S.P., 2016. Functional brain activation associated with inhibitory control deficits in older adults. Cereb. Cortex 26 (1), 12–22. doi:10.1093/cercor/bhu165, Epub 2014 Aug 1. PMID: 25085883.

Cuypers, K., Marsman, A., 2021. Transcranial magnetic stimulation and magnetic resonance spectroscopy: opportunities for a bimodal approach in human neuroscience. Neuroimage 224, 117394.

Ding, B., Chen, K.M., Ling, H.W., Zhang, H., Chai, W.M., Li, X., Wang, T., 2008. Diffusion tensor imaging correlates with proton magnetic resonance spectroscopy in posterior cingulate region of patients with Alzheimer's disease. Dement. Geriatr. Cognit. Disord. 25 (3), 218–225.

Ding, X.Q., Maudsley, A.A., Sabati, M., Sheriff, S., Schmitz, B., Schütze, M., et al., 2016. Physiological neuronal decline in healthy aging human brain - an *in vivo* study with MRI and short echo-time whole-brain1H MR spectroscopic imaging. Neuroimage 137, 45–51.

Duarte, J.M.N., Lei, H., Mlynárik, V., Gruetter, R., 2012. The neurochemical profile quantified by *in vivo* 1H NMR spectroscopy. Neuroimage 61, 342–362.

Edde, M., Leroux, G., Altena, E., Chanraud, S., 2021. Functional brain connectivity changes across the human life span: from fetal development to old age. J. Neurosci. Res. 99 (1), 236–262.

Eylers, V.V., Maudsley, A.A., Bronzlik, P., Dellani, P.R., Lanfermann, H., Ding, X.Q., 2016. Detection of normal aging effects on human brain metabolite concentrations and microstructure with whole-brain MR spectroscopic imaging and quantitative MR imaging. Am. J. Neuroradiol. 37 (3), 447–454.

Field, A., 2013. Discovering Statistics Using IBM SPSS Statistics, 5th ed. Sage, London.

Gasparovic, C., Song, T., Devier, D., Bockholt, H.J., Caprihan, A., Mullins, P.G., et al., 2006. Use of tissue water as a concentration reference for proton spectroscopic imaging. Magn. Reson. Med. 55 (6), 1219–1226.

Gao, F., Edden, R.A.E., Li, M., Puts, N.A.J., Wang, G., Liu, C., et al., 2013. Edited magnetic resonance spectroscopy detects an age-related decline in brain GABA levels. Neuroimage 78, 75–82.

García Santos, J.M., Fuentes, L.J., Vidal, J.B., Antequera, M., Torres Del Río, S., Antúnez, C., Ortega, G., 2010. Regional effects of age and sex in magnetic resonance spectroscopy. Radiologia 52 (4), 342–350 (Panama).

Grachev, I.D., Apkarian, A.V., 2001. Chemical network of the living human brain: evidence of reorganization with aging. Cogn. Brain Res. 11 (2), 185–197.

Grachev, I.D., Swarnkar, A., Szeverenyi, N.M., Ramachandran, T.S., Apkarian, A.V., 2001. Aging alters the multichemical networking profile of the human brain: an *in vivo* (1)H-MRS study of young versus middle-aged subjects. J. Neurochem. 77 (1), 292–303.

Greenhouse, I., Noah, S., Maddock, R.J., Ivry, R.B., 2016. Individual differences in GABA content are reliable but are not uniform across the human cortex. Neuroimage 139, 1–7.

Grossman, E.J., Kirov, I.I., Gonen, O., Novikov, D.S., Davitz, M.S., Lui, Y.W., et al., 2015. N-acetyl-aspartate levels correlate with intra-axonal compartment parameters from diffusion MRI. Neuroimage 118, 334–343.

Haga, K.K., Khor, Y.P., Farrall, A., Wardlaw, J.M., 2009. A systematic review of brain metabolite changes, measured with 1H magnetic resonance spectroscopy in healthy aging. Neurobiol. Aging 30 (3), 353–363.

Hagberg, A., Swart, P., S. Chult, D., 2008. Exploring network structure, dynamics, and function using networkX. United States.

Harris, J.L., Yeh, H.W., Swerdlow, R.H., Choi, I.Y., Lee, P., Brooks, W.M., 2014. High-field proton magnetic resonance spectroscopy reveals metabolic effects of normal brain aging. Neurobiol. Aging 35 (7), 1686–1694.

Harris, C.R., Millman, K.J., Van Der Walt, S.J., Gommers, R., Virtanen, P., Cournapeau, D., Oliphant, T.E., 2020. Array programming with NumPy. Nature 585, 357–362. doi:10.1038/s41586-020-2649-2.

Hermans, L., Leunissen, I., Pauwels, L., Cuypers, K., Peeters, R., Puts, N.A.J., et al., 2018. Brain GABA Levels are associated with inhibitory control deficits in older adults. J. Neurosci. 38 (36), 7844–7851.

Ion-Mărgineanu, A., Van Cauter, S., Sima, D.M., Maes, F., Sunaert, S., Himmelreich, U., Van Huffel, S., 2017. Classifying glioblastoma multiforme follow-up progressive vs. responsive forms using multi-parametric MRI features. Front. Neurosci. 10, 615.

Hunter, J.D., 2007. Matplotlib: a 2D graphics environment. Comput. Sci. Eng. 9 (3), 90–95.

Hutchinson, S., Kobayashi, M., Horkan, C., Pascual-Leone, A., Alexander, M., Schlaug, G., 2002. Age-related differences in movement representation. Neuroimage 17, 1720–1728.

IBM Corp., 2021. IBM SPSS Statistics for Windows Version 28.0.

Inuggi, A., Amato, N., Magnani, G., Gonzalez-Rosa, J., Chieffo, R., Comi, G., Leocani, L., 2011. Cortical control of unilateral simple movement in healthy aging. Neurobiol. Aging 32 (3), 524–538.

Jones, R.S., Waldman, A.D., 2004. ^{1}H-MRS evaluation of metabolism in Alzheimer's disease and vascular dementia. Neurol. Res. 26 (5), 488–495.
Katz-Brull, R., Koudinov, A.R., Degani, H., 2002. Choline in the aging brain. Brain Res. 951 (2), 158–165.
Kim, J.H., Lee, J.M., Jo, H.J., Kim, S.H., Lee, J.H., Kim, S.T., et al., 2010. Defining functional SMA and pre-SMA subregions in human MFC using resting state fMRI: functional connectivity-based parcellation method. Neuroimage 49, 2375–2386.
King, B.R., van Ruitenbeek, P., Leunissen, I., Cuypers, K., Heise, K.F., Santos Monteiro, T., et al., 2018. Age-related declines in motor performance are associated with decreased segregation of large-scale resting state brain networks. Cereb. Cortex 28 (12), 4390–4402.
Klein, J., 2000. Membrane breakdown in acute and chronic neurodegeneration: focus on choline-containing phospholipids. J. Neural. Transm. 107, 1027–1063.
Levin, O., Weerasekera, A., King, B.R., Heise, K.F., Sima, D.M., Chalavi, S., et al., 2019. Sensorimotor cortex neurometabolite levels as correlate of motor performance in normal aging: evidence from a ^{1}H-MRS study. Neuroimage 202, 116050.
Lin, A.L., Rothman, D.L., 2014. What have novel imaging techniques revealed about metabolism in the aging brain? Future Neurol. 9, 341–354.
Lind, A., Boraxbekk, C.J., Petersen, E.T., Paulson, O.B., Siebner, H.R., Marsman, A., 2020. Regional myo-inositol, creatine, and choline levels are higher at older age and scale negatively with visuospatial working memory: a cross-sectional proton MR spectroscopy study at 7 Tesla on normal cognitive ageing. J. Neurosci. 40 (42), 8149–8159.
Lind, A., Boraxbekk, C.J., Petersen, E.T., Paulson, O.B., Andersen, O., Siebner, H.R., Marsman, A., 2021. Do glia provide the link between low-grade systemic inflammation and normal cognitive ageing? a 1 H magnetic resonance spectroscopy study at 7 Tesla. J. Neurochem. 159 (1), 185–196.
Maddock, R.J., Caton, M.D., Ragland, J.D., 2018. Estimating glutamate and Glx from GABA-optimized mega-press: off-resonance but not difference spectra values correspond to press values. Psychiatry Res. Neuroimaging 279, 22–30.
Marenco, S., Meyer, C., Van Der Veen, J.W., Zhang, Y., Kelly, R., Shen, J., et al., 2018. Role of gamma-amino-butyric acid in the dorsal anterior cingulate in age-associated changes in cognition. Neuropsychopharmacology 43, 2285–2291.
Marjanska, M., McCarten, J.R., Hodges, J., Hemmy, L.S., Grant, A., Deelchand, D.K., Terpstra, M., 2017. Region-specific aging of the human brain as evidenced by neurochemical profiles measured noninvasively in the posterior cingulate cortex and the occipital lobe using h-1 magnetic resonance spectroscopy at 7 T. Neuroscience 354, 168–177.
Mayhew, S.D., Coleman, S.C., Mullinger, K.J., Can, C., 2022. Across the adult lifespan the ipsilateral sensorimotor cortex negative BOLD response exhibits decreases in magnitude and spatial extent suggesting declining inhibitory control. Neuroimage 253, 119081.
McKinney, W., et al., 2010. Data structures for statistical computing in python. In: Proceedings of the 9th Python in Science Conference, 445, pp. 51–56.
Mescher, M., Merkle, H., Kirsch, J., Garwood, M., Gruetter, R., 1998. Simultaneous *in vivo* spectral editing and water suppression. NMR Biomed. 11, 266–272.
Moffett, J.R., Ross, B., Arun, P., Madhavarao, C.N., Namboodiri, A.M., 2007. N-Acetylaspartate in the CNS: from neurodiagnostics to neurobiology. Prog. Neurobiol. 81 (2), 89–131.
Nasreddine, Z.S., Phillips, N.A., Bédirian, V., Charbonneau, S., Whitehead, V., Collin, I., et al., 2005. The Montreal Cognitive Assessment, MoCA: a brief screening tool for mild cognitive impairment. J Am. Geriatr. Soc. 53 (4), 695–699.
Oldfield, R.C., 1971. The assessment and analysis of handedness: the Edinburgh inventory. Neuropsychologia 9, 97–113.
Parsons, M.W., Li, T., Barber, P.A., Yang, Q., Darby, D.G., Desmond, P.M., et al., 2000. Combined (1)H MR spectroscopy and diffusion-weighted MRI improves the prediction of stroke outcome. Neurology 55 (4), 498–505.
Paslakis, G., Träber, F., Roberz, J., Block, W., Jessen, F., 2014. N-acetyl-aspartate (NAA) as a correlate of pharmacological treatment in psychiatric disorders: a systematic review. Eur. Neuropsychopharmacol. 24 (10), 1659–1675.
Pelosin, E., Ogliastro, C., Lagravinese, G., Bonassi, G., Mirelman, A., Hausdorff, J.M., et al., 2016. Attentional control of gait and falls: is cholinergic dysfunction a common substrate in the elderly and Parkinson's disease? Front. Aging Neurosci. 8, 104.
Pfefferbaum, A., Adalsteinsson, E., Spielman, D., Sullivan, E.V., Lim, K.O., 1999. *In vivo* spectroscopic quantification of the N-acetyl moiety, creatine, and choline from large volumes of brain gray and white matter: effects of normal aging. Magn. Reson. Med. 41 (2), 276–284.
Posse, S., Otazo, R., Dager, S.R., Alger, J., 2013. MR spectroscopic imaging: principles and recent advances. J. Magn. Reson. Imaging 37 (6), 1301–1325.
Puts, N.A., Edden, R.A., Evans, C.J., McGlone, F., McGonigle, D.J., 2011. Regionally specific human GABA concentration correlates with tactile discrimination thresholds. J. Neurosci. 31 (46), 16556–16560.
Ross, B.D., Ernst, T., Kreis, R., Haseler, L.J., Bayer, S., Danielsen, E., et al., 1998. 1H MRS in acute traumatic brain injury. J. Magn. Reson. Imaging 8 (4), 829–840.
Ross, A.J., Sachdev, P.S., Wen, W., Brodaty, H., 2006. Longitudinal changes during aging using proton magnetic resonance spectroscopy. J Gerontol. A Biol. Sci. Med. Sci. 61 (3), 291–298.
Sailasuta, N., Ernst, T., Chang, L., 2008. Regional variations and the effects of age and gender on glutamate concentrations in the human brain. Magn. Reson. Imaging 26 (5), 667–675.
Schliebs, R., Arendt, T., 2011. The cholinergic system in aging and neuronal degeneration. Behav. Brain Res. 221 (2), 555–563.
Simmonite, M., Carp, J., Foerster, B.R., Ossher, L., Petrou, M., Weissman, D.H., Polk, T.A., 2019. Age-related declines in occipital GABA are associated with reduced fluid processing ability. Acad. Radiol. 26 (8), 1053–1061.
Stevens, J.P., 1984. Outliers and influential data points in regression analysis. Psychol. Bull. 95 (2), 334–344.
Suri, S., Emir, U., Stagg, C.J., Near, J., Mekle, R., Schubert, F., et al., 2017. Effect of age and the APOE gene on metabolite concentrations in the posterior cingulate cortex. Neuroimage 152, 509–516.
Tayebati, S.K., Marucci, G., Santinelli, C., Buccioni, M., Amenta, F., 2015. Choline-containing phospholipids: structure-activity relationships versus therapeutic applications. Curr. Med. Chem. 22 (38), 4328–4340.
Träber, F., Block, W., Lamerichs, R., Gieseke, J., Schild, H.H., 2004. 1H Metabolite relaxation times at 3.0 Tesla: measurements of T1 and T2 values in normal brain and determination of regional differences in transverse relaxation. J. Magn. Reson. Imaging 19 (5), 537–545.
Tumati, S., Opmeer, E.M., Marsman, J.C., Martens, S., Reesink, F.E., De Deyn, P.P., Aleman, A., 2018. Lower choline and myo-inositol in temporo-parietal cortex is associated with apathy in amnestic MCI. Front. Aging Neurosci. 10, 106.
Urenjak, J., Williams, S.R., Gadian, D.G., Noble, M., 1993. Proton nuclear magnetic resonance spectroscopy unambiguously identifies different neural cell types. J. Neurosci. 13 (3), 981–989.
Verstraelen, S., Cuypers, K., Maes, C., Hehl, M., Van Malderen, S., Levin, O., et al., 2021. Neurophysiological modulations in the (pre)motor-motor network underlying age-related increases in reaction time and the role of GABA levels - a bimodal TMS-MRS study. Neuroimage 243, 118500.
Vints, W., Kušleikiene, S., Sheoran, S., Šarkinaite, M., Valatkevičiene, K., Gleizniene, R., et al., 2022. Inflammatory blood biomarker kynurenine is linked with elevated neuroinflammation and neurodegeneration in older adults: evidence from two ^{1}H-MRS post-processing analysis methods. Front. Psychiatry 13, 859772.
Wansapura, J.P., Holland, S.K., Dunn, R.S., Ball Jr., W.S., 1999. NMR relaxation times in the human brain at 3.0 Tesla. J. Magn. Reson. Imaging 9 (4), 531–538.
Waragai, M., Moriya, M., Nojo, T., 2017. Decreased N-Acetyl Aspartate/Myo-Inositol ratio in the posterior cingulate cortex shown by magnetic resonance spectroscopy may be one of the risk markers of preclinical Alzheimer's disease: a 7-year follow-up study. J. Alzheimers Dis. 60 (4), 1411–1427.
Weerasekera, A., Levin, O., Clauwaert, A., Heise, K.F., Hermans, L., Peeters, R., et al., 2020. Neurometabolic correlates of reactive and proactive motor inhibition in young and older adults: evidence from multiple regional ^{1}H-MR spectroscopy. Cereb. Cortex Commun. 1 (1) tgaa028.
Wijtenburg, S.A., McGuire, S.A., Rowland, L.M., Sherman, P.M., Lancaster, J.L., Tate, D.F., et al., 2013. Relationship between fractional anisotropy of cerebral white matter and metabolite concentrations measured using (1)H magnetic resonance spectroscopy in healthy adults. Neuroimage 66, 161–168.
Yang, A., Xiao, X., Wang, Z., 2014. Evaluation of normal changes in pons metabolites due to aging using turbo spectroscopic imaging. Am. Soc. Neuroradiol. 35 (11), 2099–2105.
Yousry, T.A., Schmid, U.D., Alkadhi, H., Schmidt, D., Peraud, A., Buettner, A., Winkler, P., 1997. Localization of the motor hand area to a knob on the precentral gyrus. A new landmark. Brain 120, 141–157.
Zahr, N.M., Mayer, D., Rohlfing, T., Chanraud, S., Gu, M., Sullivan, E.V., Pfefferbaum, A., 2013. *In vivo* glutamate measured with magnetic resonance spectroscopy: behavioral correlates in aging. Neurobiol. Aging 34 (4), 1265–1276.
Zhong, X., Shi, H., Shen, Z., Hou, L., Luo, X., Chen, X., et al., 2014. ^{1}H-proton magnetic resonance spectroscopy differentiates dementia with Lewy bodies from Alzheimer's disease. J. Alzheimer Dis. 40, 953–966.